Ann. Geophys., t. 31, fasc. 1, 1975, p. 69-76

The effects of different field aligned ionization models on the electron densities and total flux tube contents deduced from Whistlers*

by

M. ROTH

Institut d'Aéronomie Spatiale de Belgique
3, Avenue Circulaire, B-1 180 Brussels, Belgium

ABSTRACT. – *The total electron content of flux tubes, and the electron densities in both the equatorial plane and at the altitude of 1 000 km, have been calculated for different types of electron distributions (i.e. Diffusive Equilibrium, Constant density model, Gyro-Frequency model and Exospheric models with and without angular rotation). The results for these different models are compared with those obtained when an empirical r^{-4} model for the electron density distribution along a geomagnetic field line (where r is the geocentric radial distance) is used in the interpretation of whistler observations. It is shown that the inferred values of the equatorial densities are not so sensitive to the choice of the model as are the electron densities at 1 000 km altitude where satellite observations are available. This result may be useful for the analysis of a whistler whose propagation path cannot be experimentally specified as being either definitely inside or definitely outside the plasmapause.*

The results deduced from a given whistler observation with exospheric models, for reasonable values of the angular rotation rate, are nearly coincident with those deduced from the r^{-4} model. This good agreement between the physical exospheric models and the empirical r^{-4} model (well supported by satellite observations and whistler observations outside the plasmapause) provides a strong support for the validity of the kinetic theory of ion-exospheres.

RESUME. – *Le contenu électronique total des tubes de force, et les densités électroniques à la fois dans le plan équatorial et à l'altitude de 1 000 km, sont calculés pour différents types de distributions électroniques (c. à d. : modèle barométrique, modèle à densité constante, modèle gyrofréquence et modèles exosphériques avec et sans vitesse angulaire de rotation). Les résultats obtenus avec ces différentes distributions sont comparés aux résultats que l'on obtient lorsqu'on utilise, dans l'interprétation d'observations des siffleurs, un modèle empirique pour la distribution de densité électronique variant proportionnellement à r^{-4} (r étant la distance radiale géocentrique). On montre que les densités électroniques dans le plan de l'équateur ne sont pas aussi sensibles au choix du modèle que ne le sont les densités électroniques à 1 000 km d'altitude où l'on dispose d'observations effectuées par satellites. Ce résultat peut être utile pour l'analyse d'un siffleur dont le chemin de propagation ne peut pas être expérimentalement spécifié comme étant soit définitivement à l'intérieur, soit définitivement à l'extérieur, de la plasmapause.*

Les résultats obtenus à partir d'une observation de siffleurs, à l'aide de modèles exosphériques et pour des valeurs raisonnables de la vitesse angulaire de rotation, coïncident presque avec les résultats déduits à partir du modèle en r^{-4}. Ce bon accord entre les modèles physiques de l'exosphère et le modèle empirique en r^{-4} (bien confirmé à l'extérieur de la plasmapause, par les observations par satellites et par siffleurs) fournit une preuve pour la validité de la théorie cinétique des exosphères ioniques.

---

* Contributed paper presented at the 2d meeting of the European Geophysical Society, *Physics of the Plasmapause Symposium*, Trieste, September, 23-26, 1974.

1. Introduction

In interpreting whistler observations, an ad hoc assumption is usually made on the model for the distribution of ionization along the whistler propagation path. The purpose of this paper is to compare the results obtained when different physical and empirical models are used for the whistler analysis.

The method developed by Smith (1960, 1961b), and discussed by Helliwell (1965), is used in this paper to deduce the equatorial density, the exobase density, the total flux tube content and the equatorial distance of the field line along which the whistler has propagated. The different models considered are :

– the r^{-4} model, r being the geocentric radial distance along a geomagnetic field line,

– the constant density model (*C*),

– the diffusive equilibrium model (*DE*),

– the gyro frequency model (*GF*),

– the collisionless model of Eviatar, Lenchek and Singer (1964) for a non-rotating planet (*ELS*),

– and a similar model developed by Lemaire (1973) but including a finite rotational rate $\Omega \neq 0$(*L*).

These models are briefly described in Section 2. The whistler nose frequencies, the nose time delays and the change in the McIlwain parameter L of the whistler path are determined in Section 3 for each of these models. The equatorial density, the exobase density and the total flux tube content are calculated for these different models in Section 4. The conclusions are summarized in Section 5.

2. Description of the models

A centred dipole magnetic field is considered and only hydrogen ions are taken into account above the reference level altitude h_0. The temperatures T_0 of the thermal electrons and ions are assumed to be independent of the latitude.

2.1. The r^{-4} model (r^{-4})

The equatorial electron concentration beyond the plasmapause deduced from whistlers recorded during magnetically quiet periods decreases with McIlwain parameter L roughly as L^{-4} (Carpenter and Park, 1973 ; see also Chappell, 1972). Outside the plasmasphere, Angerami and Carpenter (1966) used an electron distribution behaving as $n_e \propto r^{-4}$ along field lines. The choice of this radial dependence is based on a comparison with the collisionless distribution described by Eviatar *et al.* (1964).

Since the empirical r^{-4} model is frequently used to represent the electron density variation outside the plasmasphere we will take it as a reference model.

2.2. The constant density model (C)

In this model it is assumed that the density remains constant along the field lines. Therefore the total tube content is simply proportional to the volume of the tube.

2.3. The diffusive equilibrium model (DE)

For diffusive equilibrium, the magnetospheric plasma is distributed according to hydrostatic equilibrium, where the partial pressure gradient is balanced by forces due to gravity and the electrostatic polarization field which is set up to prevent charge separation. Because of the magnetic field control of plasma diffusion, equilibrium conditions apply along magnetic field lines. Inside the plasmasphere this hydrostatic model is quite appropriate as a consequence of the large Coulomb collision rate (Bauer, 1969).

2.4. The gyrofrequency model (GF)

This model has been frequently used by a number of workers (Storey, 1953 ; Gallet, 1959 ; Smith, 1960, 1961a) in whistler studies. In this model, it is assumed that the field aligned electron density is proportional to the strength of the earth's magnetic field at that point (or equivalently to the local gyrofrequency). The model was therefore called the gyrofrequency model. A physical justification for this distribution was given by Dowden (1961) : an individual charged particle in the earth's magnetic field encloses a constant amount of flux in its spiral motion (Alfvén, 1950). Therefore the electron density tends to be approximately proportional to the strength of the earth's magnetic field.

2.5. The Eviatar-Lenchek-Singer exospheric model (ELS)

Following Eviatar *et al.* (1964), the ions and electrons evaporated from the top of the ionosphere are collisionless. The particle trajectories in the magnetosphere are controled by the gravitational field, the centred-dipole magnetic field and the Pannekoek-Rosseland polarization electrostatic field. All charged particles have mirror points in the collision-dominated lower regions of the ionosphere where their velocity distribution is Maxwellian. It is also assumed that the distributions of ionization at the ends of the field lines are symmetric with respect to the magnetic equator, i.e. the ionospheric densities and temperatures are the same in both hemispheres. The effect of centrifugal forces was ignored in this exospheric model. At the reference level the velocity distribution is a truncated Maxwellian with a common temperature for both the ions and electrons. Such collisionless models are justified in the region beyond the plasmapause where the density is so small that the Coulomb collisions may be neglected to a first approximation.

2.6. The Hartle model (H)

Hartle (1969) has generalized the Eviatar *et al.* collisionless model by considering non-symmetric exobase conditions. In particular, the density and/or temperature are assumed to be different at magnetically conjugate points of the exobase or reference level.

2.7. The Lemaire exospheric model (L)

The models of Eviatar *et al.* (1964) and Hartle (1969) do not include the rotation of the ionosphere-magnetosphere system. Although the centrifugal force remains small compared with the gravitational force for radial distances less than four or five earth radii, the rotational effects play a significant role in the high altitude regions along $L > 5$ field lines. For $L < L_c$ (where L_c is a critical L value related to the angular rotation speed Ω), the total potential (gravitational, electrostatic and centrifugal) has a maximum in the equatorial plane. In this case the density distribution in a symmetrical collisionless model is nearly the same as in the Eviatar *et al.* model. Along field lines with $L > L_c$, the potential is a doubly peaked function of latitude with maxima out of the equatorial plane, and a minimum at the equator. The density distribution in this case was obtained by Lemaire (1973).

Since the convection velocity of thermal plasma outside the plasmapause can be quite large, the local angular rotation speed of flux tubes can become significantly larger than the Earth's rotational speed ($\Omega_E = 7.29 \times 10^{-5}$ rad s^{-1}). In this case centrifugal forces will significantly reduce the potential energy at large radial distances.

It is important to note that for the exospheric models of Eviatar, Lenchek and Singer (1964), Hartle (1969) and Lemaire (1973), the lack of energy equipartition due to the absence of collisions and the constraint for the particles to move along magnetic field lines lead to an anisotropic velocity distribution function.

Figure 1 illustrates the electron concentrations along the $L = 7.5$ field line in the southern hemisphere for the different models described above. The reference level altitude is $h_0 = 1\,000$ km ; the reference level electron and H^+ ion concentrations were normalized to unity, and the reference level temperatures of the electrons and H^+ ions are taken equal to 1 500 K.

It can be seen that for a non-rotating *DE* model the density decreases much more slowly with increasing r than in the r^{-4} model. The *GF* model gives intermediate values of the concentration which are roughly four times larger than those of the r^{-4} model for $r < 2.2$, but become larger for $r > 2.2$. The *H*

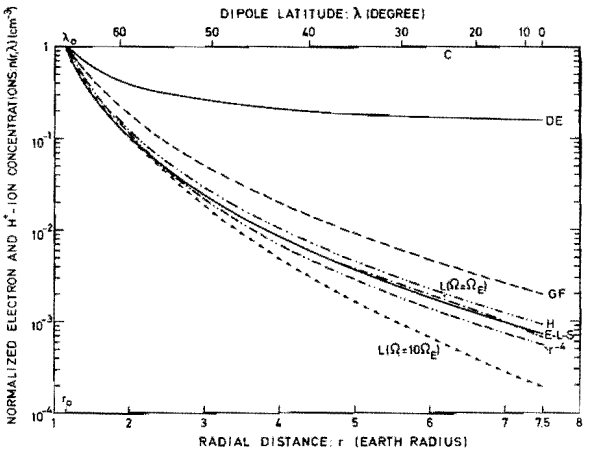

Fig. 1

Normalized electron and hydrogen ion densities in the southern hemisphere along the $L = 7.5$ field line for different models of the outer ionosphere described in Section 2. The reference level altitude is $h_0 = 1\,000$ km. For the symmetric models *DE*, *ELS* and *L*, the temperatures at the reference level are taken equal to 1 500 K. The asymmetric H model shows the $e^- - H^+$ densities for equal exobase concentrations in both hemispheres but for different exobase temperatures : $n_0^N/n_0^S = 1$, $T_0^S = 1\,500$ K, $T_0^N = 3\,000$ K.

model shows the electron concentration when the northern temperature is multiplied by a factor two compared to the southern exobase temperature ($T_0^N = 3\,000$ K and $T_0^S = 1\,500$ K). Due to the augmentation of the particle injection rate in the northern hemisphere the total number of particles in the system is higher than in the corresponding symmetric *ELS* model. The increase in the temperature at the northern exobase leads to an increase in the high-energy tail of the velocity distribution of emerging particles and a decrease in the number of low energy particles. Therefore, the relative number density just above the northern exobase is slightly diminished, whereas at higher altitudes it is increased. As a consequence of the increase of the number of particles in the high-energy tail of the velocity distribution at the northern exobase, more particles are able to pass the equatorial potential barrier, and a larger increase of the number density results in the southern hemisphere (Hartle, 1969). As we only consider symmetric distributions, the *H* model will not be taken into account in the following sections.

A distribution similar to the *ELS* distribution is obtained in the *L* model when the angular velocity Ω is equal to Ω_E, the angular rotation speed of the Earth, ($\Omega_E = 7.29 \times 10^{-5}$ rad. s^{-1}). However, when Ω increases, the collisionless density distribution decreases, and for $\Omega > 2\ \Omega_E$ the density always remains smaller than in the r^{-4} model, as can be seen in Figure 1 for $\Omega = 10\ \Omega_E$.

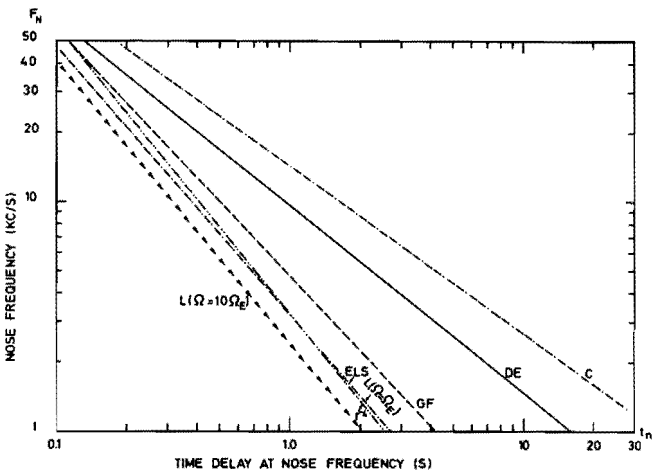

Fig. 2

Nose frequency as a function of nose time delay predicted from different models of the outer ionosphere. The reference level altitude, temperature and electron concentration are : $h_0 = 1\,000$ km, $T_0 = 1\,500$ K and $n_0 = 3\,000\,\mathrm{cm}^{-3}$.

III. Nose frequency - Time delay characteristics

The models described above have been used to compute the theoretical nose frequency (f_n) – time delay (t_n) curves illustrated in Figure 2. The paths of integration in the time delay integral are dipolar field lines above the reference level $h_0 = 1\,000$ km where the concentrations are assumed to be $n_0(e^-) = n_0(H^+) = 3\,000\,\mathrm{cm}^{-3}$; the températures are supposed to be 1 500 K. A change in n_0 would shift the curves but their slopes would remain unchanged. It can be seen that the lines corresponding to the ELS and $L(\Omega = \Omega_E)$ coincide approximately, and have a slightly smaller slope than the r^{-4} model. The slope of the $(f_n - t_n)$ curve for an exospheric model with $\Omega = 10\,\Omega_E$ is larger than that corresponding to the r^{-4} model.

The variations in the McIlwain parameter L of the whistler path from given or observed nose frequencies are given in Figure 3. These variations represent the corrections which have to be made in the prediction of the L-value when another type of electron distribution is used instead of the r^{-4} model. For $L > 3.5$, it can be seen that the C and DE models would predict smaller L-values than those given by the r^{-4} model, by factors of about 0.92 and 0.93 respectively. These corrections may be significant for large L-values. The GF model gives a L-value which is smaller than the corresponding L-value predicted with the r^{-4} model by a factor of about 0.98 at $L = 7$. The exospheric models without angular rotation and with rotational speed equal to Ω_E would predict practically the same L-values as those determined from the r^{-4} model. For a large enough rotational speed the correction becomes positive $(\Delta L > 0)$.

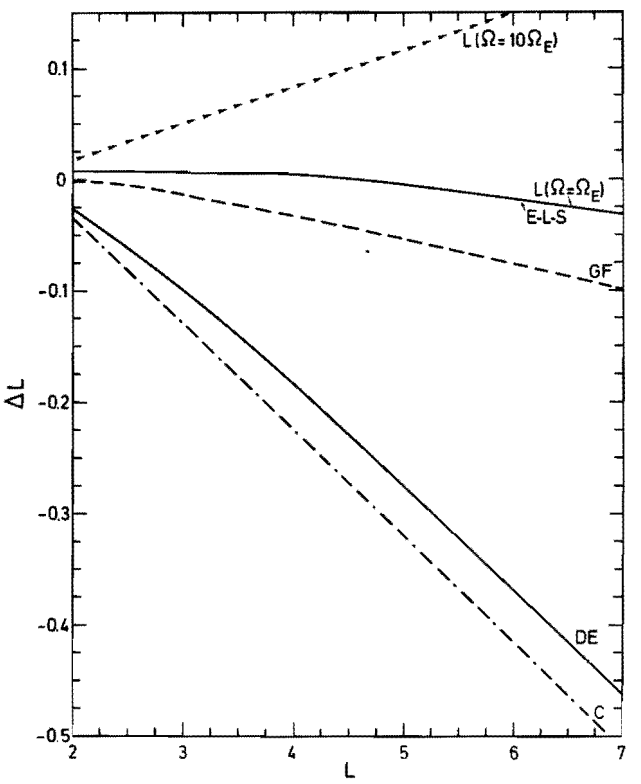

Fig. 3

Effect of the field-line model on the determination of the L-value of the whistler propagation path. ΔL is the correction which has to be added to the L-value when another type of electron distribution is used instead of the r^{-4} model.

IV. Electron densities and total tube electron contents

From a measured time delay t_n at the nose frequency f_n, it is possible to deduce the equatorial electron density $n_{eq}(L)$ for a given model of the electron distribution along the L field line. Since the r^{-4} model is often adopted in the interpretation of whistler observations, we take this model as a reference distribution and compare the results obtained for other types of models with those corresponding to the reference model.

Figure 4 shows the ratio $n^x_{eq}(L)/\bar{n}_{eq}(L)$ for similar sets of values $(f_n - t_n)$. X stands for C, DE, GF, ELS or L and the bar characterizes quantities using the r^{-4} model. This ratio corresponds to the factor by which the equatorial density calculated with the r^{-4} model should be multiplied in order to obtain

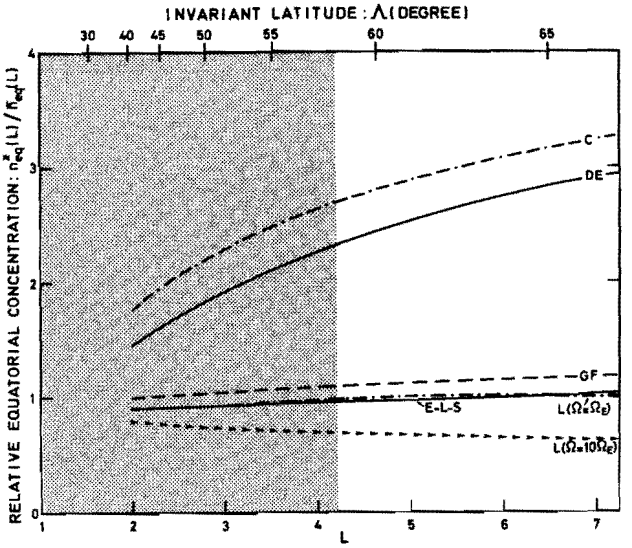

Fig. 4

Relative equatorial electron concentrations, $n^x_{eq}(L)/\bar{n}_{eq}(L)$, ($x = C, DE, GF, ELS, L$, and $- = r^{-4}$), deduced from the ($f_n - t_n$) curves of Figure 2 for the different models considered. The reference level altitude and temperature are $h_0 = 1\,000$ km and $T_0 = 1\,500$ K. The shaded area corresponds to the plasmasphere collision-dominated region. The different curves give the factor by which $\bar{n}_{eq}$ has to be multiplied when another type of electron distribution is used instead of the r^{-4} model.

the corresponding equatorial density deduced with another type of model. It can be seen that beyond 4 Earth radii, the exospheric models corresponding to $\Omega = 0$ (Eviatar, Lenchek and Singer, 1964) and $\Omega = \Omega_E$ (Lemaire, 1973) give the same results as the r^{-4} reference model. For the exospheric model with $\Omega = 10\ \Omega_E$ the equatorial densities are smaller by a factor 0.7 – 0.6 than those calculated with the r^{-4} model. The gyrofrequency model gives slightly higher values of $n_{eq}(L)$ than those deduced from the r^{-4} model. It is interesting to note that with the diffusive equilibrium model and the constant density model respectively one gets equatorial densities which are larger than those for the r^{-4} model by factors of only 2.4 and 2.8 at $L = 4.5$.

Using these equatorial electron densities it is possible to infer the corresponding electron densities $n_0(L)$ at an ionospheric level of 1 000 km where satellite measurements are available. Figure 5 illustrates the ratio $n^x_0(L)/\bar{n}_0(L)$ corresponding to the different models considered. It can be seen that for a similar set of observations ($f_n - t_n$) the dispersion of the results at 1 000 km is much more dependent on the choice of the model than in the case of Figure 4. For instance at $L = 4.5$, the constant density model or the diffusive equilibrium model would give electron densities at 1 000 km which are respectively 90 and 20 times smaller than those predicted

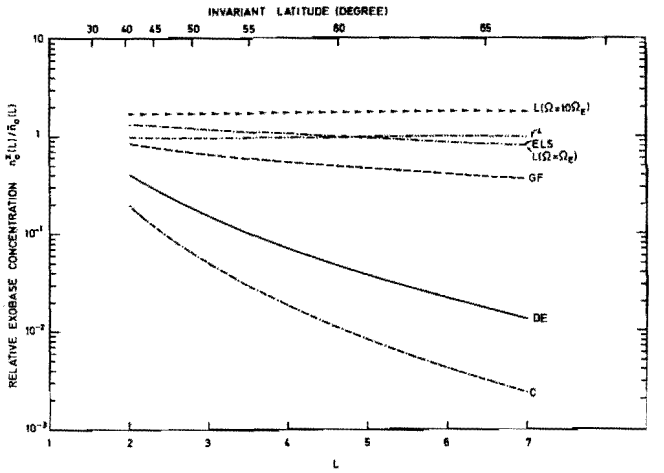

Fig. 5

Relative electron densities, $n^x_0(L)/\bar{n}_0(L)$, ($x = C, DE, GF, ELS, L$, and $- = r^{-4}$), at an ionospheric level of 1 000 km where the temperature is assumed to be 1 500 K for different models of the outer ionosphere. The different curves give the factor by which n_0 has to be multiplied when another type of electron distribution is used instead of the r^{-4} model.

with the r^{-4} reference model. The exospheric models with $\Omega = 0$ and $\Omega = \Omega_E$ predict nearly the same results as the r^{-4} model ($n^x_0/\bar{n}_0 \sim 1$). For large rotational rates, $n^L_0(L)$ is larger than $\bar{n}_0(L)$. These results may be useful for the analysis of a whistler whose propagation path cannot be experimentally specified as being either definitely inside or definitely outside the plasmapause.

For given or observed values of ($f_n - t_n$) and a given model for the electron density distribution one can also deduce the total electron content $N(L)$ of complete flux tubes above a 1 cm^2 area at an altitude of 1 000 km. Figure 6 shows the ratios $N^x(L)/\bar{N}(L)$ for the various models considered. It can be seen from this figure that the choice of a particular model is not crucial in deducing the total electron content of a flux tube since the differences between the models are less than 10 %.

IV. Conclusions

From the measurements of the nose frequency f_n and propagation time t_n of a whistler one can determine $n_{eq}(L)$, the equatorial density of electrons in the magnetosphere, $n_0(L)$, the electron density at an ionospheric altitude of 1 000 km, and $N(L)$, the total electron content of a flux tube. These values will depend on the model adopted for the electron density profile along the magnetic field lines. An empirical r^{-4} radial dependence is often used for this density distribution and has been shown to fit the observations beyond $L = 3$-4.

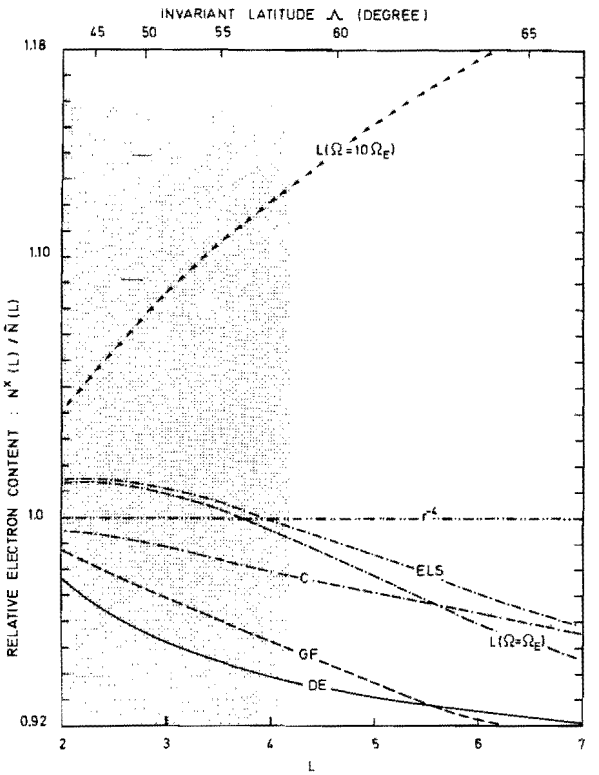

Fig. 6

Relative total tube electron contents, $N^x/\bar{N}$, ($x = C, DE, GF, ELS, L$, and $- = r^{-4}$), as a function of the McIlwain parameter L. The reference level altitude and temperature are $h_0 = 1\,000$ km and $T_0 = 1\,500$ K. The shaded area corresponds to the plasmaphere collision-dominated region. The different curves give the factor by which $\bar{N}$ has to be multiplied when another type of electron distribution is used instead of the r^{-4} model.

In this paper we consider other different types of electron density distributions, including exospheric models with an anisotropic velocity distribution function, and compare the resulting values of $n_{eq}(L)$, $n_0(L)$ and $N(L)$ with those obtained when the r^{-4} model is used. First, it is noticed (Figure 3) that the L-value deduced from an observed whistler depends on the choice of the type of electron distribution, but the L-values deduced with exospheric models are nearly the same as those obtained with the r^{-4} reference model. It is shown (Figure 4) that the equatorial density depends only moderately on the choice of the type of model, and that the collisionless model of Eviatar, Lenchek and Singer (1964) and its generalization by Lemaire (1973) to include the effect of rotation give results quite comparable to the empirical r^{-4} model.

The choice of the model has much more influence when the density at 1 000 km is deduced from a specific whistler observation. But here again the exospheric models with reasonable values of the angular rotation speed Ω give values of $n_0(L)$ which are not very different from those deduced with the r^{-4} reference model. Finally, the total electron content $N(L)$ as deduced from a set of $(f_n - t_n)$ values is rather insensitive to the type of model adopted to describe the ionization distribution in the field-aligned propagation duct of the whistler.

Acknowledgements

The author wishes to thank Professor M. Nicolet for his interest during the preparation of this paper. He is also deeply grateful to Dr. J. Lemaire for his valuable comments and his assistance in evaluating this paper.

Manuscrit reçu le 14 Décembre 1974

References

Alfven, M., *Cosmical Electrodynamics*, Oxford Univ. Press, 1950.

Angerami, J.J., and Carpenter, D.L., "Whistler Studies of the Plasmapause in the Magnetosphere, 2. Electron Density and Total Tube Electron Content near the Knee in Magnetospheric Ionization", *J. Geophys. Res.*, 71, (3), 711-725, 1966.

Bauer, S.J., "Diffusive Equilibrium in the Topside Ionosphere", *Proc. IEEE*, 57, (6), 1114-1118, 1969.

Carpenter, D.L. and Park, C.G., "On what Ionospheric Workers should know about the Plasmapause-Plasmasphere", *Rev. Geophys. Space Phys.*, **11**, 133-154, 1973.

Chappell, C.R., "Recent Satellite Measurements of the Morphology and Dynamics of the Plasmasphere", *Rev. Geophys. Space Phys.*, **10**, (4), 951-979, 1972.

Dowden, R.L., "A theoretical model of electron density along a geomagnetic line of force in the exosphere", *J. Atmos. Terr. Phys.*, **20**, 122-130, 1961.

Eviatar, A., Lenchek A.M. and Singer S.F., "Distribution of density in an ion-exosphere of a non-rotating planet", *Phys. Fluids*, 7, 1775-1779, 1964.

Gallet, R.M., "The very low frequency emissions generated in the earth's exosphere", *Proc. IRE*, 47 (2), 211-231, 1959.

Hartle, R.E., "Ion-Exosphere with Variable Conditions at the Baropause", *Phys. Fluids*, **12** (2), 455-462, 1969.

Helliwell, R.A., *Whistlers and Related Ionospheric Phenomena*, Stanford University Press, Stanford, California, 1965.

Lemaire, J., "Rotating Ion-Exospheres", *Personal communication*, 1973.

Smith, R.L., "The use of nose whistlers in the study of the outer ionosphere", *Tech. Rept.* n° 6, contract AF18(603) – **126**, Radio Sc. Lab., Stanford Univ., AFOSR TN/60-861. July 11, 1960.

Smith, R.L., "Propagation characteristics of whistlers trapped in field-aligned columns of enhanced ionization", *J. Geophys. Res.*, **66** (11), 3699-3707, 1961a.

Smith, R.L., "Properties of the outer ionosphere deduced from nose whistlers", *J. Geophys. Res.*, **66** (11), 3709-3716, 1961b.

Storey, L.R.O., "An investigation of whistling atmospherics", *Phil. Trans. Roy. Soc. (London)*, **A**, **246**, 113-141,1953.